ACS ES&T Engineering

pubs.acs.org/estengg

Article

Mechanistic Study of Arsenate Adsorption onto Different Amorphous Grades of Titanium (Hydr)Oxides Impregnated Point-of-Use Activated Carbon Block

Alireza Farsad, Kaidi Niim, Mahmut Selim Erşan, Jose Ricardo Gonzalez-Rodriguez, Kiril D. Hristovski, and Paul Westerhoff*

Cite This: ACS EST Engg 2023, 3, 989−1000

Read Online

ACCESS | Metrics & More | Article Recommendations | * Supporting Information

ABSTRACT: Millions of households still rely on drinking water from private wells or municipal systems with arsenic levels approaching or exceeding regulatory limits. Arsenic is a potent carcinogen, and there is no safe level of it in drinking water. Point-of-use (POU) treatment systems are a promising option to mitigate arsenic exposure. However, the most commonly used POU technology, an activated carbon block filter, is ineffective at removing arsenic. Our study aimed to explore the potential of impregnating carbon blocks with amorphous titanium (hydr)oxide (THO) to improve arsenic removal without introducing titanium (Ti) into the treated water. Four synthesis methods achieved 8−16 wt % Ti-loading within the carbon block with a 58−97% amorphous THO content. The THO-modified carbon block could adsorb both oxidation states of arsenic (arsenate and arsenite) in batch tests. Modified carbon block with higher Ti and amorphous content always led to better arsenate removal, achieving arsenic loadings up to 31 mg As/g Ti and 70,000 bed volumes in continuous-flow tests. Impregnating carbon block with amorphous THO consistently outperformed impregnating with crystalline TiO_2. The best-performing system (TTIP-EtOH carbon block) was amorphous THO derived using titanium isopropoxide, ethanol, and acetic acid via the sol−gel technique at 80 °C for 18 h and dried overnight at 60 °C. Comparable pore-size distribution and surface area of the impregnated carbon blocks suggested that chemical properties played a more significant role than physical and textural properties in removing arsenate via the amorphous Ti-impregnated carbon blocks. Equilibrium isotherms indicated energetically favorable adsorption for amorphous chemically synthesized adsorbents. The sized adsorption coefficients for the amorphous TTIP-EtOH carbon block were fitted using a pore-surface diffusion model, $D_{surface} = 3.1 \times 10^{-12}$ and $D_{pore} = 3.2 \times 10^{-6}$ cm²/s. Impregnating the carbon block with THO enabled effective arsenic removal from water without affecting the pressure drop across the unit or the carbon block's ability to remove pollutants efficiently and chemical

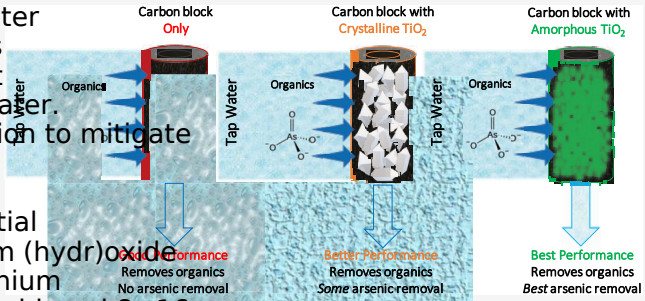

KEYWORDS: arsenate, water, titanium, adsorption, carbon block

1. INTRODUCTION

Arsenic occurs in many groundwater and surface water sources across the globe, and it is among the top 10 most violated water quality standards in the United States.[1,2] As a Class A human carcinogen, long-term exposure to arsenic-contaminated potable water has been linked to kidney, skin, liver, and bladder cancer.[3] The United States Environmental Protection Agency (USEPA) and World Health Organization (WHO) have set a maximum contaminant level (MCL) of 10 μg/L for arsenic in drinking water.[4] As a carcinogen with a high MCL relative to cancer risk (i.e., 1 in 1,000 health risk instead of 1 in 1,000,000), there is no safe level for arsenic. Arsenic arguably poses among the highest cancer risks in drinking water.[3] While drinking water systems comply with the 10 μg/L for arsenic, the regulation can be based on a very limited number of samples (e.g., less than one sample per year for small utilities), and many communities have arsenic levels near the MCL.[5] Over 40 million people in the U.S. rely upon private wells that are rarely measured and not regulated for arsenic, but drinking water arsenic exposures are known to occur.[5,6] Globally, arsenic concentrations exceeding the WHO regulations in drinking water may impact more than 200 million people.[7] Thus, reducing arsenic exposure levels in tap water remains an important societal need.

Received: January 7, 2023
Revised: March 3, 2023
Accepted: March 6, 2023
Published: March 20, 2023

https://doi.org/10.1021/acsestengg.3c00012
ACS EST Engg 2023, 3, 989−1000

Arsenic occurs in the two inorganic oxidation states of arsenate (As(V)) and arsenite (As(III)). Because of their pK_a values, arsenate occurs as a deprotonated oxo-anion at common drinking water pH levels, whereas arsenite is nonionic and more challenging to remove without an oxidation step. Many iron, aluminum, titanium, cerium, zirconium, or other metal (hydr)oxide-based adsorbents are effective in adsorbing arsenate.[8,9] The adsorbent type and pore structure significantly influence arsenate removal capability.[10,11] In the U.S.A., the commercial materials mostly used by municipalities are iron (hydr)oxide or crystalline titanium dioxide (TiO_2)-based sorbents.[12−14] Titanium (hydr)oxides (THO) are stable under environmentally relevant pH conditions[15] and can form inner-sphere complexation with arsenate through oxygen bridges.[16,17] In situ THO synthesis through hydrolysis/precipitation or sol−gel methods allow flexibility to use different procedures and titanium precursors that lead to formation of THO with different physicochemical characteristics and tunable degrees of crystallinity.[8,18,19] Because crystalline forms of THO are easier to characterize and study, amorphous THO is overlooked in research despite its arsenate removal capability.[20] Consequently, there is a gap in studying the mechanisms of arsenate immobilization by different amorphous graded THO. Furthermore, using high-surface-area (nano) powders of amorphous THO is not practical for water treatment applications due to its poor hydraulic stability or need for postfiltration to remove particulates.[21] Therefore, THO immobilization into a porous support is a prerequisite. Integration of nanostructured THO into pores of mesoscale adsorbents that have good hydraulic performance is an appropriate alternative.[22]

Activated carbon block filters are porous compact point-of-use (POU) disposable cartridges fitting into canisters under the sink and have zero liquid waste. Carbon block filters have short hydraulic retention times (<30 s), adsorb organic pollutants, and filter particulates (e.g., pathogens, colloidal lead, and copper).[23,24] Carbon blocks have a rapid mass transport from water to highly porous and high-surface-area activated carbon.[25] However, a carbon block is not designed to remove oxo-anions such as arsenate. Therefore, we explored impregnation of THO with different degrees of crystallinity into an activated carbon block to create a multifunctional POU filters that remove arsenate. Our underlying premise was that increasing the degree of amorphous synthesized THO in commercial carbon block improves arsenate removal without impacting its hydraulic behavior or ability to remove organic pollutants.

The goal of this study was to explore the relationship between the amorphous content of the THO-impregnated carbon block and arsenic removal from water in both batch- and continuous-flow experiments. The focus was on the more commonly occurring arsenate As(V) oxo-anion. Limited experiments showed the ability to also remove arsenite (As(III)). We hypothesized that (1) increasing drying temperature decreases the amorphous content of the synthesized THO and (2) arsenate adsorption capacity (μg As/g adsorbent) is positively proportional to the THO amorphous content. Four techniques were utilized to synthesize stable titanium (hydr)oxide materials within the pores of a carbon block. Pseudo-equilibrium adsorption capacity experimental data were modeled using Freundlich isotherms for use with the pore-surface diffusion model (PSDM), which provides insights into arsenic mass transport within the modified carbon block. Additionally, continuous- or intermittent-flow packed-bed column experiments were carried out to evaluate the effectiveness of the THO-impregnated carbon block in eliminating arsenate from both model and real waters and to demonstrate its practicality in real-world matrices. The possible adverse influence of the impregnation process on the intrinsic capability of the carbon block in removing organic contaminants was studied using a model polar chlorinated organic contaminant (i.e., *para*-chlorobenzoic acid (*p*CBA)).

2. METHODOLOGY

2.1. Carbon Block Impregnation Procedures.

A commercial carbon block (ACEPURE (10″ length × 4.5″ diameter, with an average particle size of 5 μm)) was selected to study the effect of the type of synthesized THO because in-house tests confirmed the following: (1) it contains negligible background titanium and (2) it does not remove arsenate in dynamic column tests. To work with a manageable size of carbon block for impregnation and reasonable quantities of water in continuous-flow tests, commercial carbon block was cut into cylindrical cores with a diameter and height of 32 and 22 mm, respectively (a bed volume (BV_{cm^3}) of 17 cm^3) using a circular drilling tool. These dimensions were selected to maintain consistency with the hydraulic loading rates and empty bed contact times (EBCT) commonly used in carbon block POU systems (loading rate of 4.5 $m^3/m^2 \cdot h$ and an EBCT of 0.28 min).[26] Carbon block cores were then impregnated with THO and used in continuous-flow experiments.

Two impregnation methods were used to understand the impact of precursors on the formation of stable THO coatings within the carbon block pores: hydrolysis/precipitation (using titanium oxysulfate (TOS) resulting in the TOS carbon block) and sol−gel (using different precursors and procedures). First, sol−gel impregnation compared the effectiveness of two different precursors, titanium isopropoxide (TTIP) or titanium butoxide (TiBu), resulting in TTIP-EtOH and TiBu-EtOH carbon blocks, respectively. Second, sol−gel impregnation using TiBu was combined with preformed commercial crystalline (anatase/rutile) titanium dioxide (Degussa P90) resulting in a P90-filled carbon block. Table S2 summarizes key synthesis conditions for the fabricated sorbents and their acronyms. The procedures from the existing literature[18,27−29] were modified to synthesize THO inside the carbon block pores (in situ). The detailed synthesis procedures are described in the Supporting Information (SI).

Using the same synthesis methods described above, instead of impregnating the carbon blocks, THO powders were produced and used for complimentary analysis, characterization, and pseudo-equilibrium batch adsorption tests. To evaluate hypothesis #1 (increasing THO drying temperature decreases the amorphous THO content), powders were collected, dried at various temperatures up to 450 °C to vary crystallinity, analyzed by an X-ray diffractometer (XRD), and evaluated for arsenate adsorption tests through batch experiments. The details for all of the employed characterization techniques are provided in the SI.

2.2. Dynamic-Flow Column Tests for Pollutant Removal.

Continuous-flow column tests were performed to investigate and compare the arsenate adsorption capacity and removal efficiency of unmodified and impregnated carbon blocks under a dynamic regime used in the POU filters. Carbon blocks were inserted into a brass holder that

https://doi.org/10.1021/acsestengg.3c00012
ACS EST Engg. 2023, 3, 989−1000

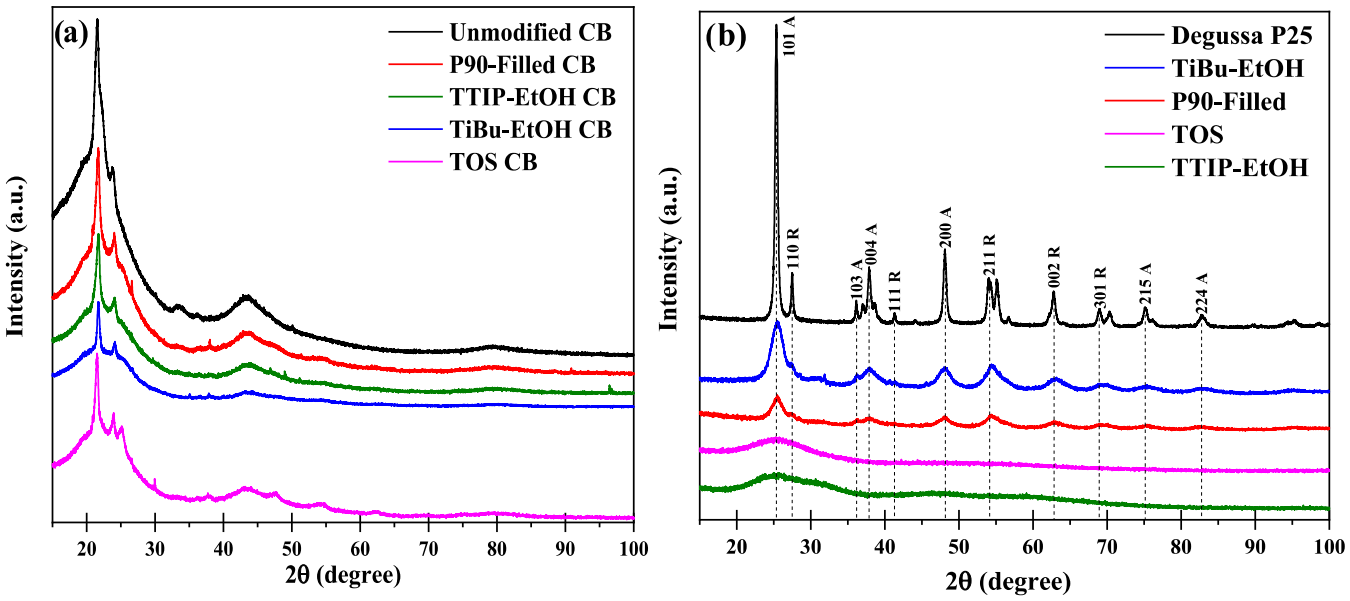

Figure 1. XRD patterns of (a) THO-impregnated carbon blocks (CBs) and (b) THO powders formed outside the porous carbon block. In the peak labels, "A" refers to anatase and "R" refers to rutile phases.

water through the carbon block (Figure S1). A QG-150 pump with a Q2 head was used to continuously flow the water. The pressure drop across the carbon block was measured using a pressure gauge installed on the column inlet. Figure S2 illustrates the apparatus used for continuous column tests. Before the experiments, the system was prewashed continuously with deionized (DI) water for 8 h to remove any residues of the side products and unreacted chemicals until a constant pH of 5−6. The flow rate was set to 60 mL/min, giving a loading rate of 7.4 m^3/m^2/h and an EBCT of 0.28 min. These loading rates and contact times are typical of carbon blocks.

First, a model water containing 1.3 μM (100 μg/L) arsenate was prepared using sodium arsenate. Because the intent of the dual-purpose adsorbent is to simultaneously remove both inorganic and organic pollutants from tap water within a single engineered device, removal of the probe organic pollutant (*p*CBA) with an initial concentration of 1.9 μM (300 μg/L) was also monitored. *p*CBA was chosen for experiments due to its polar chlorinated organic structure, which is harder to remove by activated carbon than nonpolar organics like chloroform, often used to test carbon blocks. The polar structure of *p*CBA is representative of many emerging organic pollutants or pesticides found in water.[30] pH buffer was used, but the pH of the solution did not vary during the experiment (pH = 6.3 ± 0.2 at 22 ± 1 °C). Second, after the successful proof of concept, a second set of column tests were performed in the presence of background oxo-anions (silicates, phosphates, etc.) and higher pH levels, both known to adversely influence arsenate removal by metal oxide adsorbents.[31] The background salts represent realistic ranges for drinking water, including levels above the USEPA secondary total dissolved solids level of 500 mg/L (~780 μS/cm), which is common in the southwestern U.S.A. Arsenate occurs naturally in groundwaters. Influent solutions were prepared by spiking 100 μg/L arsenate and 300 μg/L *p*CBA to the local Tempe's tap water (pH 7.8, alkalinity 160 mg/L as $CaCO_3$, and conductivity 1314 μS/cm) and 10× diluted tab water (pH 7.6, alkalinity 16 mg/L as $CaCO_3$, and conductivity 139 μS/cm). Table S3 describes the tap water chemistry. These more challenging operational conditions provided insight into the potential operational range of the modified carbon block from the most optimistic (pH 6.3 model water) to more challenging tap waters (pH 7.8 with competing ions). The pH of diluted and undiluted Tempe's tap waters did not change during the experiments due to its alkalinity.

POU systems generally operate intermittently.[32] During "off" cycles, arsenate can diffuse from the near surface of the carbon block deeper into the pores of the adsorbent, which increases the available binding sites near the outer surface of the carbon block adsorbent before an "on" cycle is initiated. Therefore, arsenate removal from the system effluent was compared for continuous- vs intermittent-flow operational modes. Since most POU systems do not operate continuously, intermittent-flow experiments were conducted to assess the effectiveness of the THO-modified carbon block. Water flowed through the carbon block for 14 h and was then turned off for 10 h. This cycle was repeated multiple times over the course of the experiment, which lasted for approximately 70,000 bed volumes. During the periods with zero flow through the carbon block, arsenic had time to diffuse into the pores of the THO-modified carbon block, leading to an increase in the number of surface sites available for arsenic adsorption when flow resumed. These experiments provide valuable insights into the limitations of arsenic mass transport within the modified carbon block. The analytical techniques used to quantify chemical species in water are detailed in the SI.

2.3. Pseudo-Equilibrium Batch Adsorption Tests.

Batch adsorption tests were performed on select samples. First, to compare the arsenate adsorption capacity of THO powders held at different drying temperatures, batch experiments were performed with an adsorbent dose of 6 mg of using 1 L polypropylene bottles filled with DI water containing 200 μg/L of arsenate and 600 μg/L of *p*CBA (pH = 6.3 ± 0.2, 22 ± 1 °C); mass concentration ratios (3 mg of *p*CBA/mg A were the same as in the dynamic-flow tests. Higher concentrations were used in batch tests because very

https://doi.org/10.1021/acsestengg.3c00012
ACS EST Engg 2023, 3, 989−1000

high adsorption capacity of the synthesized THO powder and the desire to detect >99% removal of arsenate. Second, to obtain the Freundlich isotherm parameters for use in PSDM fitting, the same batch reactors with identical concentrations and conditions were employed. THO powders (synthesized outside the carbon block) were ground, sieved with a mesh size of 170 (<90 μm), and added to bottles at doses ranging from 0.5 to 6 mg Ti/L. To confirm that samples were representative of THO inside carbon block pores, batch experiments were performed using the most amorphous THO-impregnated carbon block that was crushed after impregnation and added to bottles at doses varying from 3.5 to 40 mg/L.

The bottles were shaken for 7 days to reach pseudo-equilibrium at room temperature. Preliminary kinetic tests showed that longer than 3 days were required to reach equilibrium and no change in solution phase arsenate concentration was observed after 7 days. Arsenate and/or *p*CBA concentrations remaining in solution were fit using the Freundlich isotherm model ($q_e = K_F C_e^{1/n}$),[33] where q_e is the adsorption capacity at equilibrium (μg/mg Ti), C_e is the arsenate or *p*CBA concentration in the liquid phase at equilibrium (μg/L), K_F is the Freundlich adsorption capacity parameter (μg/mg Ti)(L/μg)$^{1/n}$, and $1/n$ is the Freundlich adsorption intensity parameter (unitless).

2.4. Pore-Surface Diffusion Model (PSDM). A MATLAB code for the PSDM developed by the Hofmann group at the University of Toronto was used to parameterize and simulate arsenate removal using the most and least amorphous THO-impregnated carbon block to study the influence of the amorphous content of the synthesized THO on the mass transport and diffusivity of the impregnated carbon block in arsenate removal. All model assumptions, equations, and correlations are provided in the SI.[34] Diffusion coefficients were parameterized over the first 10,000 BV and then used to simulate the breakthrough performance from 10,000 to 70,000 BVs.

3. RESULTS AND DISCUSSION

3.1. Crystallinity of the Synthesized Adsorbents and Effectiveness of the Coating. Figure 1a shows two XRD spectra, one for the unmodified carbon block and the other for the THO-impregnated carbon block. The unmodified carbon block XRD spectrum displays two peaks at 23 and 43°, corresponding to the (002 and 100/101) facets of carbon, respectively.[35,36] These peaks remain unchanged even after impregnation with THO. The concentration of THO inside the activated carbon pores is relatively low, so X-rays do not penetrate very deeply into the impregnated carbon block's pores. Consequently, the changes in the XRD spectra after impregnation are minimal. This low concentration of THO within the pores is due to the filter being crushed and powdered for use, causing the THO to mainly exist inside the pores of the activated carbon particles. To characterize the THO formed inside the carbon block, Figure 1b shows XRD spectra for the same THO powders produced ex situ under the same temperature, pressure, and time conditions with the same precursors and solvents as the impregnated carbon block. Broad responses from 15 to 100° indicated a lack of crystallinity of the TiO_2 for TTIP-EtOH and TOS samples. In contrast, TiBu-EtOH and P90-filled samples showed sharp diffraction peaks, more crystalline structures.

Figure S4a illustrates the XRD spectra of different synthesized THO after eliminating the background XRD signal. TTIP-EtOH had the highest amorphous content (97%), followed by TOS (95%), P90-filled (64%), and TiBu-EtOH (38%). The high amorphous content of TTIP-EtOH was attributed to the incomplete hydrolysis and smaller formed nuclei that cannot proceed to further crystallization.[37] The incomplete hydrolysis and smaller were caused by the substitution of alkoxide groups of TTIP with carboxyl groups of acetic acid during the synthesis procedure. The most amorphous THO, TTIP-EtOH, was studied further, and Figure S3a presents the XRD spectra of TTIP-EtOH dried at different temperatures. By subtracting the background and estimating the degree of crystallinity (Figure S4), analysis showed that the amorphous content of the TTIP-EtOH sample dried at 60 °C was 97% and that the amorphous content decreased to 68% for the sample dried at 450 °C. The samples dried at 150, 250, and 350 °C had amorphous contents of 91, 80, and 77%, respectively. This trend of crystallinity increasing with higher drying temperatures is consistent with the literature.[38]

Figure S5 shows the Ti-loading inside the carbon block impregnated through different procedures. The most crystalline-impregnated carbon blocks, produced via P90-filled and TiBu-EtOH syntheses, had lower Ti-loadings (8.6 and 9.3 wt %, respectively). In contrast, Ti-loadings of the amorphous TTIP-EtOH and TOS carbon blocks were 15.9 and 12.2 wt %, respectively. This higher Ti-loading could be attributed to the stabilized TiO^+ ions due to the acid present in the synthesis procedure and the well-controlled viscosity and reactivity of the precursor solution, which contained acetic acid. The acidic catalyst in some cases, mixing the titanium precursor with acetic acid in the first synthesis step, leads to the replacement of the alkoxide groups with carboxylic groups that makes it a more controllable for binding and coating purposes.[28,29] Amorphous metal oxides likely coat the media surface more homogeneously than crystalline particles.[39]

Cross-sectional scanning electron microscopy (SEM) images and energy-dispersive X-ray spectroscopy (EDX) elemental mapping were acquired from different impregnated carbon blocks (Figures S6 and S7). On the basis of Figure S6b, THO inside the TOS carbon block existed as agglomerates and chains of THO particles. In contrast, Figure S6e shows that THO particles inside the TTIP-EtOH carbon block were not agglomerated, potentially leading to more accessible arsenate adsorption sites. A high-magnification image of the TTIP-EtOH carbon block (Figure S6e) shows individual THO nanoparticles with diameters of 20 to 50 nm, which are an order of magnitude smaller than THO particles in the TiBu-EtOH carbon block (Figure S6c). The smaller THO particles in the TTIP-EtOH carbon block may result in higher surface areas and pore structures that facilitate intraparticle diffusion of arsenate. On the basis of EDX elemental mapping in Figure S7, all of the sol−gel driven impregnated carbon blocks had an even surface distribution of THO particles, while THO distribution in the TOS carbon block was more heterogeneous and had agglomerated particles. Overall, the sol−gel-based methods resulted in a more homogeneous THO surface coating due to the in situ condensation and polymerization steps of the sol−gel technique.

3.2. Arsenate Removal Performance in Dynamic Column Tests with Unmodified and THO-Impregnated Carbon Blocks. Figure 2 shows arsenate breakthrough curves for unmodified and THO-impregnated carbon blocks. Arsenate breakthrough (10,000 BV of treated water was

https://doi.org/10.1021/acsestengg.3c00012
ACS EST Engg. 2023, 3, 989−1000

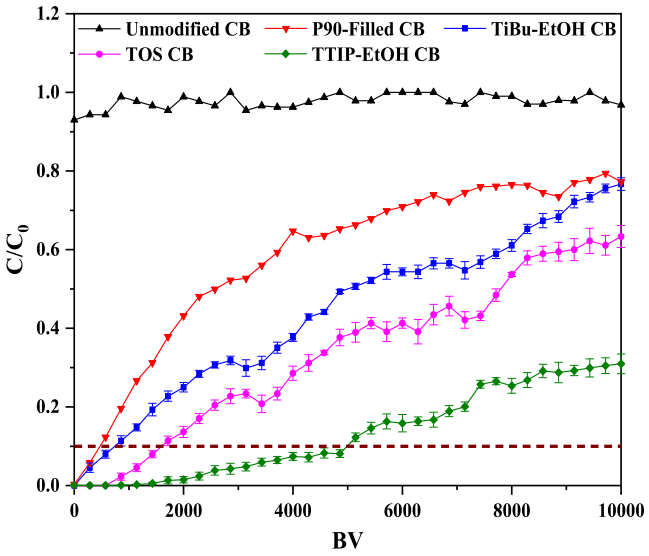

Figure 2. Arsenate removal breakthrough curves of unmodified and impregnated carbon blocks (CBs). Background matrix: DI water with arsenate = 100 μg/L, *p*CBA = 300 μg/L, pH = 6.3, and temperature = 22 ± 1 °C. Experimental conditions: EBCT = 0.28 min and loading rate = 4.5 $m^3/m^2 \cdot h$. The horizontal dashed line represents the current MCL of arsenic (10 μg/L).

used to compare the treatment performance because 5,000−10,000 L is the typical operational life recommended by POU vendors for carbon blocks having a 1 L capacity. THO impregnation did not affect the pressure/head loss through the carbon block. The pressure loss for all impregnated and unmodified carbon blocks was below 0.3 bar (1 bar = 14.5 psi), while the difference between unmodified and impregnated carbon blocks was ≤0.1 bar. Maintaining the pressure is important so that customers do not experience low flow rates. SEM images confirmed that impregnated carbon blocks had open macropores and pathways and the impregnation process did not impair the porosity structure in ways that would cause more fluid shear, drag, or other resistance to flowing water.

The highly porous carbon block provides open access to adsorption sites for arsenate. The distribution of micro-, meso-, and macropores was determined using the Barrett−Joyner−Halenda (BJH) method associated with the liquid N_2 physisorption isotherms at 77 K, presented in Figure S8 and Table S4 for the adsorption leg. The results show that mesopores (>2 and <50 nm) dominated both unmodified and impregnated carbon blocks, followed by micropores (≤2 nm). Only a small fraction (less than 10%) of the pore volume was associated with macropores (≥50 nm up to 200 nm). This distribution of pore sizes allows for efficient arsenate adsorption from water, with access to various pore sizes to accommodate the different sizes of arsenate ions. Figure 2 shows that there was near instantaneous arsenate breakthrough (i.e., no arsenate removal) for the unmodified carbon block. In all cases, impregnating THO into the carbon block improved arsenate removal. The best arsenate removal capacity was achieved by the amorphous TTIP-EtOH carbon block, followed by TOS, TiBu-EtOH, and P90-filled carbon blocks. A carbon block alone removed essential zero arsenate. Clearly, by increasing titanium loading inside the carbon block during impregnation, arsenate adsorption and removal elevate. Therefore, the obtained adsorption capacities were also normalized to the Ti-loading inside the impregnated carbon block. Table S5 summarizes the adsorption capacities normalized and not-normalized to the Ti-loading after 10,000 BVs were treated. The Ti-normalized arsenate adsorption capacity ranged from 5.7 to 8.1 mg As/g Ti. The amorphous TTIP-EtOH carbon block achieved the highest adsorption capacity (8.1 mg As/g Ti after 10,000 BV and 31 mg As/g Ti after 70,000 BV treated), nearly 40% better than the crystalline-based P90-filled carbon block. Both of the chemically synthesized impregnation methods were more promising than the P90-filled carbon block that contained commercial crystalline TiO_2.

Using titanium-based adsorbents offers a significant advantage in terms of solubility, especially compared to the iron used in other commonly used arsenate adsorbent minerals. Iron has a secondary regulatory level in drinking water due to its aesthetic properties, but this is not the case for titanium. However, because of concerns about the possible toxicity of TiO_2,[40] Ti leaching from impregnated carbon blocks was measured by analyzing column effluent samples. Ti concentrations in the effluents ranged from 12 to 22 μg/L, beginning of the column test, but less than 1 μg/L during the adsorption process, as shown in Figure S9. Overall, mass balance calculations using concentration and volumetric flow concluded that only 0.01 to 0.03% of the loaded Ti on the carbon block was released into the column effluent (Figure S9).

The second tested hypothesis was that the arsenate adsorption capacity (μg As/g adsorbent) is positively proportional to the THO amorphous content. Most prior studies focus on crystalline structure and the impact of crystalline facets on arsenate adsorption.[8,9] One possibility for the superior performance of amorphous metal(hydr)oxide adsorbents, including those synthesized using TTIP-EtOH, is that the randomness of the structure and different spatial organization of the Ti and O atoms result in different surface factors as compared to the crystalline structures, thus improving the adsorptive removal of arsenate.[8] Another reason may relate to the surface area and pore structure. Table S6 presents the Brunauer−Emmett−Teller (BET) surface area of THO powder synthesized ex situ to the carbon block preparation. The unmodified carbon block had a slightly higher surface area (371 m^2/g) than the impregnated blocks (363−447 m^2/g). Among the impregnated samples, the TTIP-EtOH carbon block had the lowest surface area (363 m^2/g) but showed the highest surface area (318 m^2/g) among the ex situ produced powders (TOS had 260 m^2/g, TiBu-EtOH had 193 m^2/g, P90-Filled had 171 m^2/g). Pore-size distributions are provided in Figure S8 and based on the BJH model. Table S6 shows the distribution of pores into micro-, meso-, and macropores. Because of the possible inaccuracies of the BJH-derived pore-size distribution,[41] the non-local density functional theory (NLDFT) model is often considered more suitable for characterizing micropores, Figure S8 includes this data. Collectively, these results indicate that THO contains >20% more micropores than crystalline P90-modified samples. TOS and TiBu-EtOH powders show the highest ratio of micropores (31% and 18%, respectively), which correlates with the arsenic removal efficiency consistently following the order of the materials' micropore ratio and surface area. Overall, the higher amorphous content based upon XRD and surface area for TTIP-EtOH-synthesized materials supported the literature showing amorphous

https://doi.org/10.1021/acsestengg.3c00012
ACS EST Engg. 2023, 3, 989−1000

structures have a higher surface area and pore volume, which results in higher adsorption site density relative to their corresponding crystalline species.[20,42]

Intuitively, the net lower surface area and pore volume of the TTIP-EtOH carbon block could have been expected to cause lower arsenate removal capacity in the dynamic column tests compared with other impregnation methods, but the opposite trend was observed. However, considering only the amorphous precipitate, which occurred within the carbon block, the TTIP-EtOH-synthesized THO had more surface area than the other synthesized powders. Thus, on a systems scale (i.e., carbon block), the chemical properties of amorphous THO appeared to have more influence than the physical properties (i.e., pore volume or surface area).

3.3. Cyclic Operation of the Impregnated Carbon Block. Because POU systems operate in on−off cycles, the best-performing impregnated carbon block (TTIP-EtOH) was tested in a cyclical mode to compare the performance against the continuous operation mode. As shown in Figure 3 (SI),[37] arsenate

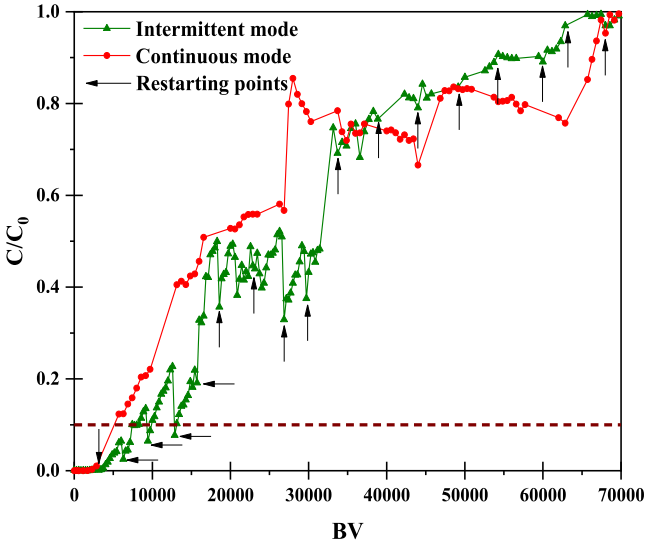

Figure 3. Arsenate breakthrough curves of TTIP-EtOH carbon block in intermittent and continuous modes. Background matrix: DI water with arsenate = 100 μg/L as As, pCO_2 = 300 μg/L, pH = 6.3, and temperature = 22 ± 1 °C. Experimental conditions: EBCT = 0.28 min and loading rate = 4.5 m^3/m^2·h. The horizontal dashed line represents the current MCL of arsenic (10 μg/L).

removal improved during cyclic operations. Arrows in Figure 3 indicate periods when the flow through the system was intermittently turned off. Upon restarting the flow, 10−20% lower effluent arsenate concentrations occurred. During periods of no flow (off-cycle stagnation periods), arsenate that had adsorbed near the outer surface of the impregnated carbon block had time to diffuse deeper in the adsorbent pores and surfaces. At 40% arsenate breakthrough (C/C_0 = 0.4), TTIP-EtOH carbon block's arsenate adsorption capacity (3.3 mg As/g carbon block) during cyclical testing was 50% greater than during continuous flow (1.5 mg As/g carbon block), showing the improved capability to remove arsenic from water. In the later stages of arsenate breakthrough (C/C_0 = 0.8), the performance difference lessened between the two operation modes, where the adsorption capacity in cyclic operation (3.3 mg As/g carbon block) was only slightly greater than in continuous operation (2.9 mg As/g carbon block), as the adsorbent approached equilibrium with influent arsenate concentrations. The driving force from water to the media reduced due to saturated adsorption sites. However, during each phase of the column operation and before reaching 10 μg/L (i.e., current arsenic MCL), the slope of the breakthrough curve for intermittent operation was shallower than that for continuous operation, and the adsorption capacity was 67% higher with intermittent operation.

3.4. Role of Retained Organic Groups in the Formation of Amorphous THO and Coordinated Oxygen in Amorphous THO-Impregnated Carbon Blocks. Figure S10 presents Fourier-transform infrared (FT-IR) spectra of the amorphous TTIP-EtOH carbon block compared with the unmodified carbon block. These spectra indicate the presence of more organic carboxylic groups on the TTIP-EtOH carbon block that justifies the formation of amorphous THO due to incomplete hydrolysis, as discussed before, which agrees with the literature (more discussion is provided in the SI).[37] Although FT-IR is only a surface characterization tool, observing carboxyl groups in the TTIP-EtOH carbon block is evidence of increased oxygen and hydroxyl groups after impregnation. Oxygen atoms have different binding energies in carboxyl groups and metal oxides. This likely benefits arsenate adsorption because the primary mechanism for arsenate removal is inner-sphere complexation through oxo bridging, and higher oxygen content of the adsorption sites improves net arsenate adsorption.[8,9] Our FT-IR data agrees with the literature that amorphous THO has more surface oxygen and hydroxyl groups.[20] In addition, functionalization with the carboxylic group as an agent appears to play a pivotal role in obtaining a more amorphous adsorbent. The increased surface oxygen group content is not only important for arsenate adsorption, but also for arsenite removal. As a proof concept to explore As(III) and As(V) removal, which is being explored in more depth currently, an equal dose of amorphous TTIP-EtOH was utilized for batch adsorption with the model water (1.35 μM (100 μg/L) [As(III)]$_0$ [As(III)]$_0$ at pH = 7.9). Figure S11 shows that TTIP-EtOH has an adsorption capacity of 21 mg of As(V)/g Ti and 18 mg As(III)/g Ti, which shows the capability of amorphous TTIP-EtOH to remove both arsenic species. Commonly, adsorbents have a lower arsenite adsorption capacity or rate because As(III) is nonionic at near-neutral pH levels. The surface oxygen groups of our THO-modified adsorbents likely facilitate the removal of arsenic via inner-sphere complexation with both arsenic redox state species (i.e., arsenate and arsenite). Figure S11 shows the X-ray photoelectron spectroscopy (XPS) O 1s spectra of TTIP-EtOH before and after arsenate and arsenite adsorption. The increased relative area under the Ti−OH peak from 20 to 9% for arsenate and 12% for arsenite, respectively, and the increase in the bridging oxygen peak by 21% imply the adsorption of both arsenate species through oxygen bridging. An increase in C−OH and C═O peaks' relative area after arsenic adsorption also suggests the surface oxygen group participation in arsenic adsorption. Overall, the mechanism of arsenic adsorption by amorphous THO involves inner-sphere complexation through oxygen bridging, wherein the surface oxygen groups and content of the adsorbent play an important role in the removal of both arsenate and arsenite.

3.5. Batch Arsenate Removal Tests, Freundlich Isotherms, and PSDM Parameterization. Simulating arsenate breakthrough in continuous-flow experiments re-

https://doi.org/10.1021/acsestengg.3c00012
ACS EST Engg. 2023, 3, 989−1000

Table 1. Fitted Freundlich Isotherm Parameters for Arsenate and *p*CBA and Pore Surface Diffusion Model Parameters for Arsenate Adsorption by TTIP-EtOH and TiBu-EtOH from Batch- and Continuous-Flow Tests

	Freundlich isotherm parameters						PSDM parameters		
	As(V)			*p*CBA			As(V)		
	$1/n$	K (μg/mg Ti)(L/μg)$^{1/n}$	R^2	$1/n$	K (μg/mg Ti)(L/μg)$^{1/n}$	R^2	D_s (cm^2/s)	D_p (cm^2/s)	Bi$_c$
TTIP-EtOH	0.23	10.9	0.95	2.34	5.2×10^{6}	0.82	3.1×10^{-12}	3.2×10^{-6}	32
TiBu-EtOH	0.25	6.8	0.94	2.87	1.6×10^{7}	0.92	0.28×10^{-12}	1.5×10^{-6}	50

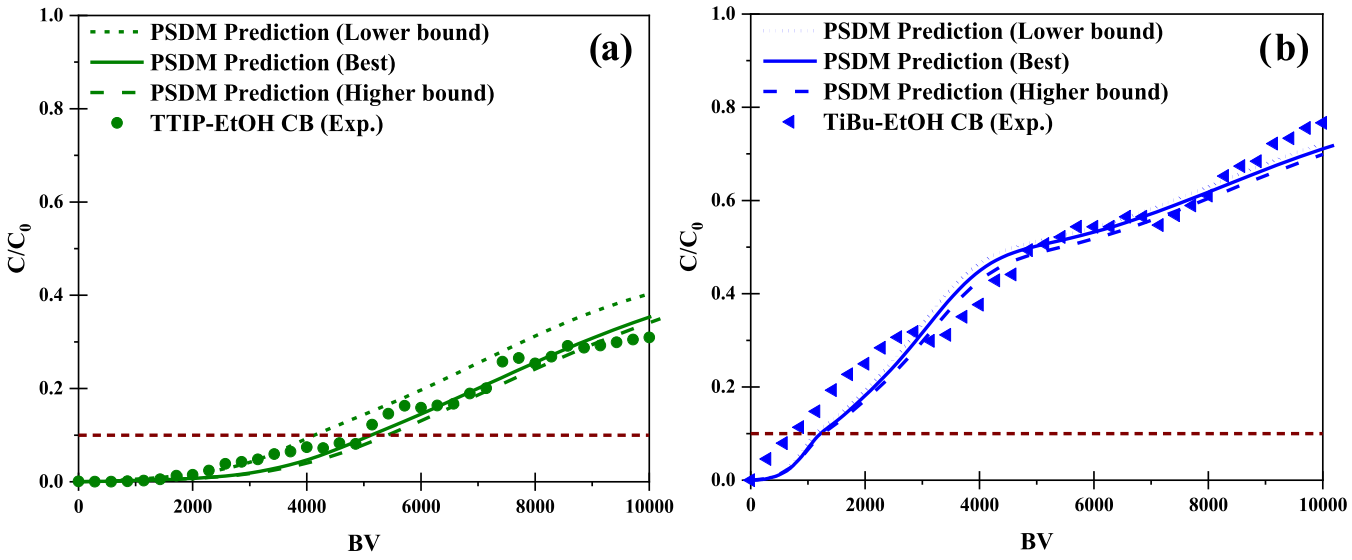

Figure 4. Observed (symbols) and PSDM predictions (lines) for arsenate breakthrough using (a) the TTTP-EtOH carbon block EtOH carbon block. Experimental and operating conditions same as provided in Figures 2 and 3. The horizontal dashed line MCL of arsenic (10 μg/L).

determining the pseudo-equilibrium adsorption capacity that serves as the driving force for diffusion into carbon block pores and surfaces. Figure S12 shows the experimental data and fitted Freundlich isotherms ($q_e = KC_e^{1/n}$) for arsenate adsorption by the different THO powders formed ex situ to the carbon block. Table 1 summarizes the fitted values. Freundlich intensity parameters ($1/n$), the most amorphous (TTIP-EtOH) and least amorphous (TiBu-EtOH) synthesized adsorbents were 0.23 and 0.25, respectively. Adsorption processes are thermodynamically favorable when the Freundlich $1/n$ values are below unity ($1/n < 1$). An $1/n = 1$ adsorption isotherm is represented by linear, uniform affinity among all surface binding sites. Values of $1/n < 1$ (i.e., sometimes expressed as $n > 1$) indicate higher heterogeneity on the adsorbent surface and the presence of numerous binding sites with varying strengths. This results in a high potential for the adsorption of the target compound from a wide range of concentrations. In simpler terms, a lower $1/n$ value implies more favorable energetics and greater effectiveness at lower chemical potentials, making it efficient for removing compounds at lower concentrations.[43] Favorable $1/n$ for TTIP-EtOH and TiBu-EtOH could be attributed to the numerous binding sites available on the surface of sol−gel-derived adsorbents. Because $1/n$ values are nearly equivalent, we can compare the Freundlich adsorption capacity (K) of both materials. Freundlich K values of amorphous TTIP-EtOH (10.9 (μg/mg Ti)(L/μg)$^{1/n}$) were 60% higher than semicrystalline TiBu-EtOH (6.8 (μg/mg Ti)(L/μg)$^{1/n}$). Parallel experiments were performed using THO powders collected ex situ to the carbon blocks as well as Ti-containing solids synthesized in situ within the carbon block pores; the block sample was crushed and sieved with a mesh size of 170 (<90 μm), and fitted in batch adsorption tests. The in situ synthesized and crushed TTIP-EtOH carbon block yielded a $1/n$ of 0.23 and K of 1.7 (μg/mg modified carbon block)(L/μg)$^{1/n}$ and 12.8 (μg/mg Ti)(L/μg)$^{1/n}$. The similar $1/n$ and K values between powders and the crushed carbon block co the validity of using THO precipitates to represent THO on the carbon block for the batch experiments. The better performance of amorphous TTIP-EtOH over semicrystalline TiBu-EtOH particulates in batch experiments is consistent with the higher arsenate removal observed in dynamic col tests with TTIP-EtOH and TiBu-EtOH carbon blocks (Figure 2). Also, the SI provides further information on the arsenate adsorption capacities of TTIP-EtOH dried at different temperatures that hold varying amorphous content.

Using Freundlich isotherms obtained from batch experiments, Figure 4a,b show the PSDM model fitting the experimental arsenate breakthrough curves for TTIP-EtOH and TiBu-EtOH carbon blocks, respectively. Upper and lower bounds on the PSDM parameterization are provided. Detai the PSDM parameterization are provided in the SI. Table S7 summarizes the key values. Significant insights can be obtained by analyzing fitted parameters and dimensionless variables from the models.[8,10] Larger intraparticle mass transport limitations are observed within the TiBu-EtOH carbon block compared to the TTIP-EtOH carbon block whe considering the fitted surface or pore diffusion coefficients (D_s or D_p) and associated combined Biot numbers (Bi_c) (Table 1). Compared with the TiBu-EtOH carbon block, with D_s

https://doi.org/10.1021/acsestengg.3c00012
ACS EST Engg 2023, 3, 989−1000

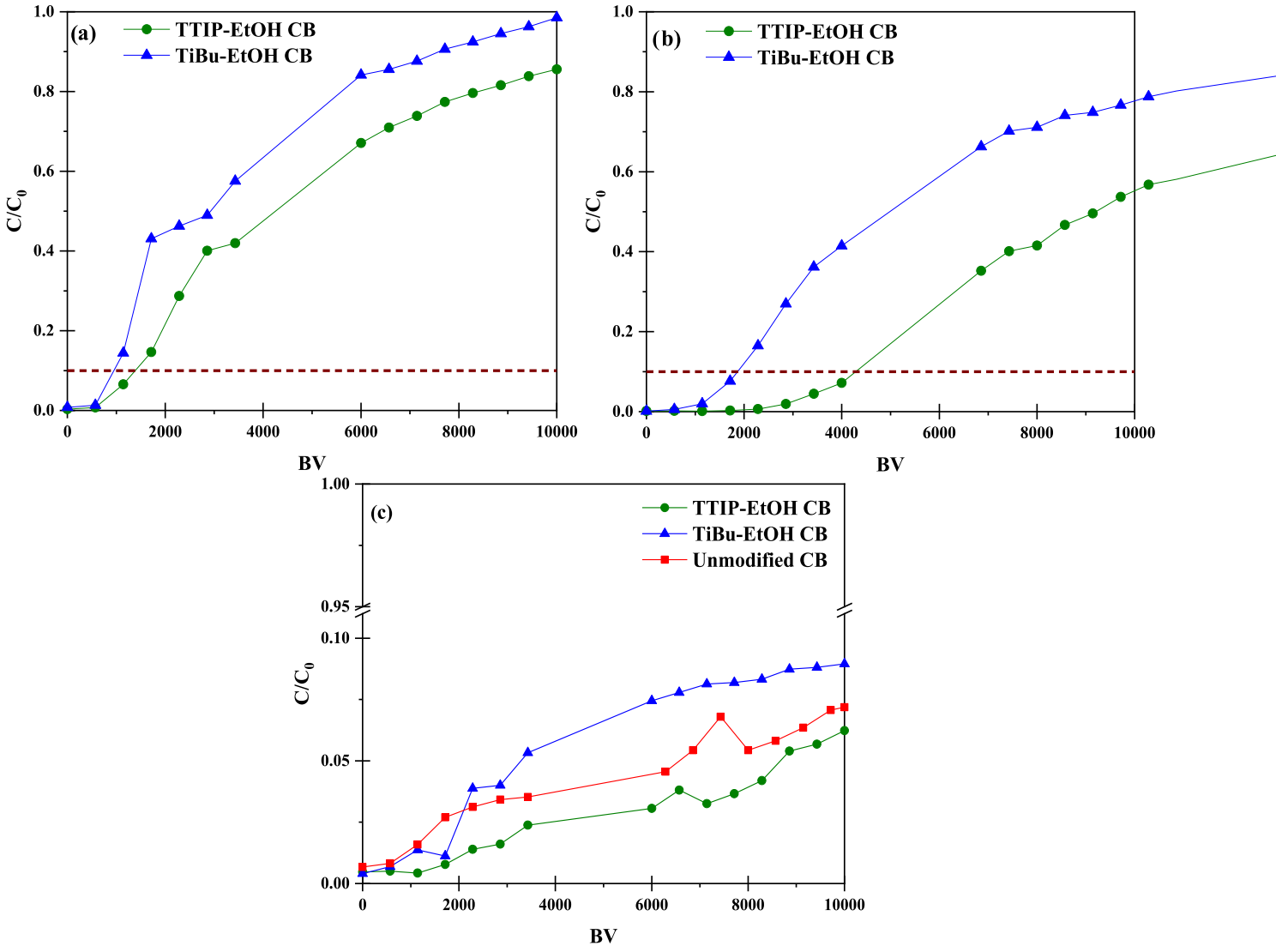

Figure 5. Pollutant breakthrough curves of TTIP-EtOH and TiBu-EtOH carbon blocks (CBs) in different water matrices: (a) arsenate breakthrough curves at conductivity = 1314 μS/cm and pH = 7.8, (b) arsenate breakthrough curves at conductivity = 139 μS/cm and pH = 7.8, and (c) *p*CBA breakthrough curves at conductivity = 1314 μS/cm and pH = 7.8 and comparison with unmodified CB performance. All CBs had the same initial arsenate (100 μg/L), *p*CBA (300 μg/L), temperature (22 ± 1 °C), EBCT (0.28 min), and loading rate (4.5 m^3/m^2·h). The horizontal dashed line represents the current MCL of arsenic (10 μg/L).

D_p values of 0.28×10^{-13} and 1.5×10^{-10} cm^2/s, respectively, D_s and D_p values for the TTIP-EtOH carbon block were ~11 and ~2 times higher, respectively ($D_s = 3.1 \times 10^{-12}$ cm^2/s and $D_p = 3.2 \times 10^{-6}$ cm^2/s), which indicates greater intraparticle diffusion within the TTIP-EtOH carbon block.[44] Impregnated carbon blocks with TTIP-EtOH showed higher arsenate adsorption efficiency, likely due to their amorphous nature. Although TIP-EtOH carbon blocks had more micropores and fewer mesopores than TiBu-EtOH carbon blocks (Table S4), pore-size distribution alone does not entirely determine adsorption efficiency. The amorphous nature of the impregnating agent, THO, probably results in higher diffusion coefficients because of the smaller particle size and more accessible surface adsorption sites. The literature suggested that for Biot numbers between 1 and 100, both film mass transfer and intraparticle diffusion are important.[45] The data sets for both carbon blocks (Table 1) had Biot numbers >20. Because higher values indicate greater importance of intraparticle mass transport,[46] this implies intraparticle diffusion controlled the overall mass transport of the system. The combined higher equilibrium adsorption capacity (K) for TTIP-EtOH created a large concentration-based driving force for arsenate in water to diffuse into the modified carbon block and reduced the net intraparticle diffusion mass transport limitations (i.e., lower Biot # for TTIP-EtOH carbon blocks).

3.6. Influence of Background Water Matrices on Arsenate and *p*CBA Removal

Figure 5a,b shows arsenate breakthrough using TTIP-EtOH or TiBu-EtOH carbon blocks for local tap water (conductivity = 1314 μS/cm) and 10-times diluted tap water (conductivity = 139 μS/cm) matrices spiked with the same arsenate levels. Arsenate removal was less efficient in the tap water with higher salts and background competing ions. The TTIP-EtOH carbon block with an arsenate adsorption capacity of 4.1 mg/g Ti over a 10,000 BV treatment still performed better than the TiBu-EtOH carbon block (~2.0 mg/g Ti), which shows superior performance of amorphous THO compared with semicrystalline THO regardless of the

https://doi.org/10.1021/acsestengg.3c00012
ACS EST Engg 2023, 3, 989−1000

background salts. Table S5 summarizes arsenate adsorption capacities after treating 10,000 BV of these initial arsenate removal column tests in DI water at pH = 6.3 showed the superior performance of amorphous TTIP-EtOH carbon with a 40% higher capacity arsenic removal capability compared with the partially crystalline P90-filled carbon block, subsequent tap water experiments only evaluated the TTIP-EtOH carbon block. Arsenate removal capability was only slightly lower (25−30%) for the TTIP-EtOH carbon block in the tap water (pH = 7.6−7.8; undiluted or 10-times diluted to a reduced conductance) compared to DI water experiments (Figure 2). This shows a promising performance of amorphous THO-impregnated carbon block in removal of arsenate from real drinking water matrices at realistic pH values and the presence of competing anions. Additional field studies will be needed to examine broader ranges of potential water qualities.

Arsenate breakthrough curves (Figure 5a,b) were steeper in the presence of higher background salts, which shows instantaneous competition between arsenate and co-occurring anions for adsorption onto THO. The tap water phosphate concentration was 6 μg/L as P (Table S3), which was very low compared to arsenate and unlikely to compete for adsorption with arsenate spiked at 6-times higher molar ratio (i.e., 7 μmole As/μmole P). As such, dissolved silicate is most likely to be the dominant competing anion during arsenate adsorption by metal(hydr)oxides.[47] The silica concentrations were 3.7 and 0.39 mg-Si/L in the tap water and 10-times diluted tap water, respectively, this corresponds to 85 and 8.6 μmole Si/μmole As, respectively. Silica concentrations above 1 mg-Si/L can significantly affect arsenate removal.[48] While silicate polymers and oligomers have a strong affinity to the THO surface, its corresponding monomers and dimers are not serious inhibitors for arsenate adsorption because arsenate has a higher surface affinity and can replace monomers and dimers.[47] Less polymerization likely occurs at lower silicate concentrations, and therefore arsenate removal efficiency is less affected at lower silicate concentrations. Other ions present in real water samples can have an adverse effect on arsenate ion adsorption. Sulfate ions, for instance, have a lower surface binding affinity on metal oxide surfaces than arsenate ions. Previous studies have shown a less than 10% reduction in arsenate adsorption in the presence of elevated sulfate levels.[9,49,50] However, in the tap water experiments conducted in this study, sulfate levels were roughly 1,000 times higher than arsenate levels, which could result in some sulfate ion competition or binding to noncompeting surface sites on THO. Additionally, cations such as Ca^{2+} and Mg^{2+} can also adsorb onto the THO surface, affecting surface charge and promoting electrostatic attraction between arsenate and adsorbent surface.[49]

The tap water pH (7.6−7.8) was higher than that of the DI water (pH = 6.3). This higher pH affects the arsenate speciation, making it occur mainly in the form of $HAsO_4^{2-}$ rather than $H_2AsO_4^-$ based on the pK_a values of arsenate (pK_{a1} = 2.3 and pK_{a2} = 6.9). The pH_{PZC} values for TTIP-EtOH and TiBu-EtOH carbon blocks were 4.5 and 5.1, respectively. While carbonate ions do not significantly compete with arsenate for adsorption, their coadsorption on the THO surface can shift the ζ-potential to lower values, resulting in greater electrostatic repulsion of arsenate ions from the surface. An increased negative charge of the adsorbent's surface along with the speciation of arsenate at higher pH leads to more electrostatic repulsion between the adsorbent and adsorbate that adversely affects the adsorption. Overall, the decline in THO performance in the tap water matrix is likely attributable to the higher pH and oligomerization and polymerization of the silicate on the metal(loid)oxide surface, which occupies the adsorption sites and inhibits the arsenate adsorption.

A model organic pollutant was also spiked into the tap waters to evaluate the influence of THO impregnation on organic pollutant removal performance of carbon block. Figure 5c shows *p*CBA removal in the tap water experiments. Without THO impregnation, *p*CBA was low (C/C_0 > 0.7) in the carbon block effluent at 10,000 BV treated, resulting in a *p*CBA adsorption capacity of 2.3 mg/g carbon block. Impregnating THO did not adversely influence the shape of the *p*CBA breakthrough curve or its adsorption capacity. *p*CBA adsorption capacities were 2.4 and 2.2 mg/g carbon block for TTIP-EtOH and TiBu-EtOH carbon blocks, respectively. This finding is consistent with our prior work showing trichloroethylene (TCE) removal was unaffected by iron impregnation of granular activated carbon.[51] The TTIP-EtOH impregnation coats only portions of the carbon block's surface (Figure S7), leaving carbon surfaces and open pores available for organic contaminant adsorption.

Additional batch experiments with *p*CBA were performed using THO powders to confirm maximum adsorption capacity by the THO itself and predominant adsorption capacity by activated carbon for *p*CBA removal. Figure S13 shows the batch experiment data and the linearized Freundlich isotherm obtained for adsorptive removal of *p*CBA with powdered TTIP-EtOH and TiBu-EtOH. There was unfavorable adsorption of *p*CBA with the synthesized THO; $1/n_F$ values were above 1, and K_F values were small, as mentioned in Table 1. As shown in Figure S14, *p*CBA removal by the THO carbon block was not affected significantly by the background water chemistry and occurrence of salts, that *p*CBA removal occurred mainly by unmodified carbon block surfaces and by the added THO. This is because the silicate in tap water polymerizes on the THO surface and not on the carbon surface. SI provides additional FT-IR characterization and discussion for *p*CBA removal. Overall, these results support the ability to engineer modified carbon block to achieve the dual purpose of simultaneously removing oxo-anion and organic contaminants from water without impairing the characteristics of the carbon block.

4. SUMMARY AND CONCLUSIONS

Carbon block is the most widely used component in POU filters, but it cannot remove arsenic from water. Our results demonstrated that sol−gel methods create amorphous THO within the pores of the activated carbon that enables the commercial carbon block to remove arsenate, and even arsenite. The best-performing synthesis method (TTIP-EtOH) involved a sol−gel method using TTIP, EtOH, and acetic acid through aging at 80 °C and drying at 60 °C, achieved a 15.9 % wt loading of Ti into carbon block and achieved arsenic adsorption capacities of 8 to >31 mg As/g in dynamic column tests (after 10,000 or 70,000 bed volumes of operation, respectively). THO impregnation resulted in a negligible additional pressure drop (<0.1 bar) through the carbon block and <0.03 wt % titanium leaching with respect to the initial Ti loading. The slight reduction (25%) in As(V) removal from tap water containing competing ions and higher pH (7.6), relative to more optimistic As(V) removal

https://doi.org/10.1021/acsestengg.3c00012
ACS EST Engg. 2023, 3, 989−1000

model water (pH = 6.3) without other competing ions is impressive and shows promise for real-world applications.

Two hypotheses were supported with experimental and modeling data. First, higher percentages of amorphous THO were achieved at lower synthesis temperatures. Second, higher percentages of amorphous THO in powders and within the carbon block improved arsenate removal in batch- and dynamic-flow carbon block tests. Finally, impregnating carbon block with THO up to ~15 wt % titanium appeared to only coat a portion of activated carbon without clogging pores. Consequently, arsenate diffusion into the hybridized carbon block could be modeled using the pore surface diffusion model wherein the THO controlled arsenate removal from water and the non-THO coated activated carbon remained available for adsorption of organic pollutants.

While crystalline metal oxides are widely used to study adsorption mechanisms, in part because of their relative ease in characterization compared amongst amorphous materials, it appears that there is tremendous opportunity to improve arsenic removal through focusing more on amorphous adsorbents rather than crystalline ones. Because amorphous THO on carbon blocks create unique surface binding sites, this novel material shows ability to remove both As(V) and As(III). The unique ability to remove arsenite is now the focus of a separate paper. The mechanisms and energetics of ion adsorption by amorphous adsorbents can play a determining role in designing novel adsorbents or retrofitting the current technologies for commercial implementation.

ASSOCIATED CONTENT

Supporting Information

The Supporting Information is available free of charge at https://pubs.acs.org/doi/10.1021/acsestengg.3c00012.

Materials and reagents; impregnation procedure details; materials characterizations and analytical methods; effect of crystallinity; PSDM details; and FT-IR discussion (PDF)

AUTHOR INFORMATION

Corresponding Author

Paul Westerhoff − *School of Sustainable Engineering and the Built Environment, Arizona State University, Tempe, Arizona 85287, United States; Nanosystems Engineering Research Center for Nanotechnology-Enabled Water Treatment; School of Sustainable Engineering and the Built Environment, Arizona State University, Tempe, Arizona 85287, United States*; orcid.org/0000-0002-9241-8759; Email: p.westerhoff@asu.edu

Authors

Alireza Farsad − *School of Sustainable Engineering and the Built Environment, Arizona State University, Tempe, Arizona 85287, United States; Nanosystems Engineering Research Center for Nanotechnology-Enabled Water Treatment; School of Sustainable Engineering and the Built Environment, Arizona State University, Tempe, Arizona 85287, United States*; orcid.org/0000-0002-1227-0011

Ken Niimi − *School of Sustainable Engineering and the Built Environment, Arizona State University, Tempe, Arizona 85287, United States; Nanosystems Engineering Research Center for Nanotechnology-Enabled Water Treatment; School of Sustainable Engineering and the Built Environment, Arizona State University, Tempe, Arizona 85287, United States*; orcid.org/0000-0001-6544-1665

Mahmut Selim Ersan − *School of Sustainable Engineering and the Built Environment, Arizona State University, Tempe, Arizona 85287, United States; Nanosystems Engineering Research Center for Nanotechnology-Enabled Water Treatment; School of Sustainable Engineering and the Built Environment, Arizona State University, Tempe, Arizona 85287, United States*; orcid.org/0000-0003-0495-0903

Jose Ricardo Gonzalez-Rodriguez − *School of Sustainable Engineering and the Built Environment, Arizona State University, Tempe, Arizona 85287, United States; Nanosystems Engineering Research Center for Nanotechnology-Enabled Water Treatment; School of Sustainable Engineering and the Built Environment, Arizona State University, Tempe, Arizona 85287, United States; Environmental Protection Research School of Chemistry, Instituto Tecnologico de Costa Rica, Cartago, 30109, Costa Rica*

Kiril D. Hristovski − *The Polytechnic School, Arizona State University, Mesa, Arizona 85212, United States; Nanosystems Engineering Research Center for Nanotechnology-Enabled Water Treatment; School of Sustainable Engineering and the Built Environment, Arizona State University, Tempe, Arizona 85287, United States*; orcid.org/0000-0001-8694-4712

Complete contact information is available at: https://pubs.acs.org/10.1021/acsestengg.3c00012

Author Contributions

CRediT: Alireza Farsad conceptualization, investigation, methodology, writing-original draft, writing-review & editing; Ken Niimi investigation, methodology, software, visualization, writing-original draft; Mahmut Selim Ersan data curation, methodology, writing-review & editing; Jose Ricardo Gonzalez-Rodriguez investigation, methodology, writing-original draft, writing-review & editing; Kiril D. Hristovski conceptualization, methodology, validation, writing-review & editing; Paul Westerhoff conceptualization, funding acquisition, investigation, project administration, supervision, writing-original draft, writing-review & editing.

Notes

The authors declare no competing financial interest.

ACKNOWLEDGMENTS

The original PSDM MATLAB code was developed by Ron Hofmann (University of Toronto). This work was partially funded by the National Science Foundation Engineering Education and Centers (EEC-1449500) and CBET (GCR 2021147) programs. The authors acknowledge the use of facilities within the Eyring Materials Center at Arizona State University supported in part by the National Science Foundation (NNCI-ECCS-1542160). This research reported was partially supported by the National Institute of Environmental Health Sciences through the Metals and Metal Mixtures: Cognitive Aging, Remediation, and Exposure Sources (MEMCARE) Center [P42ES033719]. Content is solely the responsibility of the authors and does not necessarily represent the official views of the National Institutes of Health. Laurel Passantino provided technical editing.

REFERENCES

(1) Abejón, R.; Garea, A. A Bibliometric Analysis of Research on Arsenic in Drinking Water during the 199−2012 Period: An Outlook to Treatment Alternatives for Arsenic Removal. *J. Water Process Eng.* 2015, *6*, 105−119.

(2) Allaire, M.; Wu, H.; Lall, U. National Trends in Drinking Water Quality Violations. *Proc. Natl. Acad. Sci. U.S.A.* 2018, *115*, 2078−2083.

(3) Foster, S. A.; Pennino, M. J.; Compton, J. E.; Leibowitz, S. G.; Kile, M. L. Arsenic Drinking Water Violations Decreased across the United States Following Revision of the Maximum Contaminant Level. *Environ. Sci. Technol.* 2019, *53*, 11478−11485.

(4) Podgorski, J.; Berg, M. Global Threat of Arsenic in Groundwater. *Science* 2020, *368*, 845−850.

(5) Flanagan, S. V.; Spayd, S. E.; Procopio, N. A.; Chillrud, S. N.; Braman, S.; Zheng, Y. Arsenic in Private Well Water Part 1 of 3: Impact of the New Jersey Private Well Testing Act on Household Testing and Mitigation Behavior. *Sci. Total Environ.* 2016, *562*, 999−1009.

(6) Hutson, S. S.; Barber, N. L.; Kenny, J. F.; Linsey, K. S.; Lumia, D. S.; Maupin, M. A. *Estimated Use of Water in the United States in 2000*; U.S. Geological Survey Circular: Reston, Virginia, 2004.

(7) Uppal, J. S.; Zheng, Q.; Le, X. C. Arsenic in Drinking Water − Recent Examples and Updates from Southeast Asia. *Curr. Opin. Environ. Sci. Health* 2019, *7*, 126−135.

(8) Hristovski, K. D.; Markovski, J. Engineering Metal (Hydr)Oxide Sorbents for Removal of Arsenate and Similar Weak-Acid Oxyanion Contaminants: A Critical Review with Emphasis on Factors Governing Sorption Processes. *Sci. Total Environ.* 2017, *598*, 258−271.

(9) Pincus, L. N.; Rudel, H. E.; Petrović, P. V.; Gupta, S.; Westerhoff, P.; Muhich, C. L.; Zimmerman, J. Exploring the Mechanisms of Selectivity for Environmentally Significant Oxo-Anion Removal during Water Treatment: A Review of Common Competing Oxo-Anions and Tools for Quantifying Selective Adsorption. *Environ. Sci. Technol.* 2020, *54*, 9769−9790.

(10) Luo, J.; Fu, K.; Yu, D.; Hristovski, K. D.; Westerhoff, P.; Crittenden, J. C. Review of Advances in Engineering Nanomaterial Adsorbents for Metal Removal and Recovery from Water: Synthesis and Microstructure Impacts. *ACS ES&T Eng.* 2021, *1*, 623−661.

(11) Luo, J.; Yu, D.; Hristovski, K. D.; Fu, K.; Shen, Y.; Westerhoff, P.; Crittenden, J. C. Critical Review of Advances in Engineering Nanomaterial Adsorbents for Metal Removal and Recovery from Water: Mechanism Identification and Engineering Design. *Environ. Sci. Technol.* 2021, *55*, 4287−4304.

(12) Westerhoff, P.; de Haan, M.; Martindale, A.; Badruzzaman, M. Arsenic Adsorptive Media Technology Selection Strategies. 2006, http://iwaponline.com/wqrj/article-pdf/41/2/171/230081/wqrjc0410171.pdf.

(13) Nguyen, V. L.; Chen, W. H.; Young, T.; Darby, J. Effect of Interferences on the Breakthrough of Arsenic in Rapid Small-Scale Column Tests. *Water Res.* 2011, *45*, 4069−4080.

(14) Gingerich, D. B.; Sengupta, A.; Barnett, M. O. Is the Arsenic Rule Affordable? *J. Am. Water Works Assoc.* 2017, *109*, E381−E392.

(15) Hu, S.; Shi, Q.; Jing, C. Groundwater Arsenic Adsorption on Granular TiO_2 Integrating Atomic Structure, Filtration, and Health Impact. *Environ. Sci. Technol.* 2015, *49*, 9707−9713.

(16) Westerhoff, P.; Highfield, D.; Badruzzaman, M.; Yoon, Y. Rapid Small-Scale Column Tests for Arsenate Removal in Iron Oxide Packed Bed Columns. *J. Environ. Eng.* 2005, *131*, 262−271.

(17) Yamani, J. S.; Miller, S. M.; Spaulding, M. L.; Zimmerman, J. B. Enhanced Arsenic Removal Using Mixed Metal Oxide Impregnated Chitosan Beads. *Water Res.* 2012, *46*, 4427−4434.

(18) Garcia, J.; Markovski, J.; Gifford, J. M.; Apul, O.; Hristovski, K. D. The Effect of Media (Hydr)Oxide Nano-Enabling on Intraparticle Mass Transport of Organic Contaminants in Hybrid Granular Activated Carbon. *Sci. Total Environ.* 2017, *586*, 1219−1227.

(19) MacWan, D. P.; Dave, P. N.; Chaturvedi, S. A Review on Nano-TiO_2 Sol-Gel Type Syntheses and Its Applications. *J. Mater. Sci.* 2011, *46*, 3669−3686.

(20) Jegadeesan, G.; Al-Abed, S. R.; Sundaram, V.; Choi, H.; Scheckel, K. G.; Dionysiou, D. D. Arsenic Sorption on TiO_2 Nanoparticles: Size and Crystallinity Effects. *Water Res.* 2010, *44*, 965−973.

(21) Miller, S. M.; Zimmerman, J. B. Novel, Bio-Based, Photoactive Arsenic Sorbent: TiO_2-Impregnated Chitosan Bead. *Water Res.* 2010, *44*, 5722−5729.

(22) Elton, J.; Hristovski, K.; Westerhoff, P. Titanium Dioxide-Based Hybrid Ion-Exchange Media for Contaneous Removal of Arsenic and Nitrate. In *ACS Symposium Series*; ACS Publications, 2013; pp 223−236.

(23) Wu, C.-C.; Love, N. G.; Olson, T. M. Bacterial Transmission and Colonization in Activated Carbon Block (ACB) Point-of-Use (PoU) Filters. *Environ. Sci.: Water Res. Technol.* 2017, *3*, 1114−1124.

(24) Chen, B.; Jiang, J.; Yang, X.; Zhang, X.; Westerhoff, P. Roles and Knowledge Gaps of Point-of-Use Technologies for Mitigating Health Risks from Disinfection Byproducts in Tap Water: A Critical Review. *Water Res.* 2021, *200*, No. 117265.

(25) Kim, J.; Morgott, A.; Wu, Z.; Hopaluk, L.; Miles, M.; Stoner, W.; Li, Q. In *Simulating Transport and Adsorption of Organic Contaminants in 3D Porous Activated Carbon Blocks*; ICOMS Media, Conference, 2019.

(26) Lee, H. *Improving Activated Carbon Performance in Point Of Use and Municipal Processes*; Arizona State University, 2018.

(27) da Fonseca, B. T.; D'Elia, E.; Siqueira, J. M., Jr.; de Oliveira, S. M.; dos Santos Castro, K. L.; Ribeiro, E. S. Study of the Characteristics and Properties of the $SiO_2/TiO_2/Nb_2O_5$ Material Obtained by the Sol−Gel Process. *Sci. Rep.* 2021, *11*, No. 1106.

(28) Bahtat, A.; Bouazaoui, M.; Bahtat, M.; Garapon, C.; Jacquier, B.; Mugnier, J. Up-Conversion Fluorescence Spectroscopy in Er^{3+} TiO_2 Planar Waveguides Prepared by a Sol-Gel Process. *J. Non-Cryst. Solids* 1996, *202*, 16−22.

(29) Doeuff, S.; Henry, M.; Sanchez, C.; Livage, J. Hydrolysis of Titanium Alkoxides: Modification of the Molecular Precursor by Acetic Acid. *J. Non-Cryst. Solids* 1987, *89*, 206−216.

(30) Richardson, S. D.; Ternes, T. A. Water Analysis: Emerging Contaminants and Current Issues. *Anal. Chem.* 2018, *90*, 398−428.

(31) Dabizha, A.; Bahr, C.; Kerstel, M. Predicting Breakthrough of Vanadium in Fixed-Bed Absorbent Columns with Complex Groundwater Chemistries: A Multi-Component Granular Ferric Hydroxide vanadate−arsenate−phosphate Adsorption System. *Water Res. X* 2020, *9*, No. 100061.

(32) Clark, G. G.; Pan, W.; Giammar, D. E.; Nguyen, T. H. Influence of Point-of-Use Filters and Stagnation on Water Quality in Preschool and under Laboratory Conditions. *Water Res.* 2022, *211*, No. 118034.

(33) Freundlich, H. Über Die Adsorption in Lösungen. *Z. Phys. Chem.* 1907, *57U*, 385−470.

(34) Friedman, G. Mathematical Modeling of Multicomponent Adsorption in Batch and Fixed-Bed Reactors. Master's Thesis; Michigan Technological University, 1987.

(35) Wibawa, P. J.; Nur, M.; Asy'ari, M.; Nur, H. SEM, XRD and FTIR Analyses of Both Ultrasonic and Heat Generated Activated Carbon Black Microstructures. *Heliyon* 2020, *6*, No. e03546.

(36) Girgis, B. S.; Temerk, Y. M.; Gadelrab, M. M.; Abdullah, D. X-Ray Diffraction Patterns of Activated Carbons Prepared under Various Conditions. *Carbon Lett.* 2007, *8*, 95−100.

(37) Hanaor, D. A. H.; Chironi, I.; Karatchevtseva, I.; Triani, G.; Sorrell, C. C. Single and Mixed Phase TiO_2 Powders Prepared by Excess Hydrolysis of Titanium Alkoxides. *Adv. Appl. Ceram.* 2012, *111*, 149−158.

(38) Martin, N.; Rousselot, C.; Rondot, D.; Palmino, F.; Mercier, R. Microstructure Modification of Amorphous Titanium Oxide Thin Films during Annealing Treatment. *Thin Solid Films* 1997, *300*, 113−121.

https://doi.org/10.1021/acsestengg.3c00012
ACS EST Engg 2023, 3, 989−1000

(39) Deng, M.; Wu, X.; Zhu, A.; Zhang, Q.; Liu, Q. Well-Dispersed TiO_2 Nanoparticles Anchored on Fe3O4 Magnetic Nanosheets for Efficient Arsenic Removal. *J. Environ. Manage.* 2019, *237*, 63−74.
(40) Caloudova, H.; Blahova, J.; Mares, J.; Richtera, L.; Franc, A.; Garajova, M.; Tichy, F.; Lenz, J.; Caloudova, J.; Enevova, V.; Kopel, P.; Havelkova, B.; Lakdawala, P.; Svobodova, Z. The Effects of Dietary Exposure to Magnéli Phase Titanium Suboxide and Titanium Dioxide on Rainbow Trout (Oncorhynchus Mykiss). *Chemosphere* 2022, *293*, No. 133689.
(41) de Lange, M. F.; Vlugt, T. J. H.; Gascon, J.; Kapteijn, F. Adsorptive Characterization of Porous Solids: Error Analysis Guides the Way. *Microporous Mesoporous Mater.* 2014, *200*, 199−215.
(42) Rao, P.; Sun, Z.; Zhang, W.; Yao, W.; Wang, L.; Ding, G. Preparation and Application of Amorphous Fe-Ti Oxides for Arsenic Removal. *RSC Adv.* 2015, *5*, 89545−89551.
(43) Markovski, J.; Hristovski, K. D. An Experimental Approach for Determining Thermodynamic Surface Complexation Descriptors of Weak-Acid Oxyanions onto Metal (Hydr)Oxides: Case Study of Arsenic and Titanium Dioxide. *Sci. Total Environ.* 2019, *677*, 167−174.
(44) Hand, D. W.; Crittenden, J. C.; Thacker, W. E. Simplified Models for Design of Fixed-Bed Adsorption Systems. *J. Environ. Eng.* 1984, *110*, 440−456.
(45) Traegner, U. K.; Suidan, M. T. Parameter Evaluation for Carbon Adsorption. *J. Environ. Eng.* 1989, *115*, 109−128.
(46) Sontheimer, H.; Crittenden, J. C.; Summers, R. S. *Activated Carbon for Water Treatment*; American Water Works Association, 1988; Vol. *115*.
(47) Hu, S.; Yan, W.; Duan, J. Polymerization of Silicate on TiO_2 and Its Influence on Arsenate Adsorption: An ATR-FTIR Study. *Colloids Surf. A* 2015, *469*, 180−186.
(48) Meng, X.; Bang, S.; Korfiatis, G. P. Effects of Silicate, Sulfate, and Carbonate on Arsenic Removal by Ferric Chloride. *Water Res.* 2000, *34*, 1255−1261.
(49) Zhang, W.; Liu, C.; Wang, Z.; Zheng, T.; Ren, G.; Li, J.; Ma, J.; Zhang, G.; Song, H.; Zhang, Z.; Li, Z. A Novel Nanostructured Fe-Ti-Mn Composite Oxide for Highly Efficient Arsenic Removal: Preparation and Performance Evaluation. *Colloids Surf. A* 2019, *561*, 364−372.
(50) Jézéquel, H.; Chu, K. H. Removal of Arsenate from Aqueous Solution by Adsorption onto Titanium Dioxide Nanoparticles. *J. Environ. Sci. Health, Part A* 2006, *41*, 1519−1528.
(51) Cooper, A. M.; Hristovski, K.; Möller, T.; Westerhoff, P.; Sylvester, P. The Effect of Carbon Type on Arsenic and Trichloroethylene Removal Capabilities of Iron (Hydr)Oxide Nanoparticle-Impregnated Granulated Activated Carbon. *J. Hazard. Mater.* 2010, *183*, 381−388.

https://doi.org/10.1021/acsestengg.3c00012
ACS EST Engg. 2023, 3, 989−1000